

Electroweak phase transition in an extension of the standard model with a real Higgs singlet

S.W. Ham⁽¹⁾, Y.S. Jeong⁽²⁾, and S.K. Oh^(1;2)

⁽¹⁾ Center for High Energy Physics, Kyungpook National University
Daegu 702-701, Korea

⁽²⁾ Department of Physics, Konkuk University, Seoul 143-701, Korea

Abstract

The Higgs potential of the standard model with an additional real Higgs singlet is studied in order to examine if it may allow the strongly first order electroweak phase transition. It is found that there are parameter values for which this model at the one-loop level with finite temperature effect may allow the desired phase transition. Those parameter values also predict that the masses of the neutral scalar Higgs bosons of the model are consistent with the present experimental bound, and that their productions in e^+e^- collisions may be searched at the proposed ILC with $\sqrt{s} = 500$ GeV in the near future.

I. Introduction

The possibility of baryogenesis by means of electroweak phase transition has recently been widely examined, since the electroweak baryogenesis can in principle be tested in the future accelerator experiments [1]. If the electroweak phase transition is strongly first order, it can fulfill the departure from thermal equilibrium which is one of the three conditions required by Sakharov that are necessary for the dynamic generation of the baryon asymmetry during the evolution of the universe [2]. It has already been observed that in the standard model (SM) the electroweak phase transition cannot be strongly first order unless the mass of the scalar Higgs boson is smaller than its lower bound set experimentally by LEP [3]. The sufficient strength of the first order electroweak phase transition is essential for preserving the generated baryon asymmetry at the electroweak scale. In the literature, a number of articles have been devoted to study the possibility of accommodating the strongly first order electroweak phase transition in various models beyond the SM [4].

Among them, an interesting possibility has been investigated several years ago, where an extension of the SM with a real Higgs singlet field has been adopted within the context of the electroweak phase transition [5]. We consider that model is inspiring, because adding a real Higgs singlet field is the simplest extension of the Higgs sector of the SM. In that model, the strength of the first order electroweak phase transition has been stronger than that in the case of the SM. Due to the presence of cubic terms in the tree-level Higgs potential, a strongly first order electroweak phase transition has been ensured for a scalar Higgs boson mass of around 100 GeV, for the top quark mass of 150 GeV.

In this paper, we would like to reexamine the model in a more rigorous way, in the sense that we perform the full integration of the finite-temperature effective potential instead of approximating it up to second order in temperature, that we include the Higgs contributions to the finite temperature Higgs potential at the one-loop level, and that we take into account the zero-temperature one-loop Higgs potential. As the experimental lower bound on the scalar Higgs boson mass by now is improved to be more than 114 GeV, and the top quark mass is usually set as about 175 GeV, we would like to explore the parameter space of the model, with these new numbers in mind, where the first order electroweak phase transition may be strong enough. We find that the model is able to produce strongly first order electroweak phase transition for some parameter regions where a scalar Higgs boson may have a mass larger than 114 GeV. Further, we calculate cross sections for scalar Higgs productions in e^+e^- collisions.

II. The Higgs Potential

Let us consider the Higgs potential proposed by Ref. [5] where one real Higgs singlet field is introduced to the SM Higgs sector. We follow the notations of Ref. [5]. Thus, the Higgs potential consists of one complex Higgs doublet field and one real Higgs singlet field S . The tree-level Higgs potential is given by

$$V^0(\Phi; S) = -\mu^2 \Phi^\dagger \Phi + \frac{\lambda}{4} (\Phi^\dagger \Phi)^2 + \frac{\kappa}{2} S^2 - \frac{\eta}{3} S^3 + 2\alpha (\Phi^\dagger \Phi) S^2 + \frac{\beta}{2} (\Phi^\dagger \Phi) S; \quad (1)$$

where μ , λ , κ , and η are parameters with mass dimension, and the rest are dimensionless. We assume that μ , λ , κ , and β have a positive values. The real part of the neutral component of the Higgs doublet field is, as in the SM, going to develop the non-zero vacuum expectation

value (VEV) $u = \frac{P}{2}$ while the Higgs singlet field $v = hS$. The tree-level values for u and v are determined by the extremum conditions

$$\frac{\partial V^0(u;v)}{\partial u} = \frac{\partial V^0(u;v)}{\partial v} = 0 \quad (2)$$

where

$$V^0(u;v) = \frac{1}{4}u^4 - \frac{1}{2}u^2 + \frac{1}{4}v^4 - \frac{1}{2}v^2 - \frac{1}{3}v^3 + \frac{1}{2}u^2v^2 - \frac{1}{4}u^2v \quad (3)$$

The above extremum conditions are satisfied if

$$\begin{aligned} 2 &= u^2 + v^2 - \frac{1}{2}v; \\ \frac{2}{s} &= sv^2 + u^2 - \frac{1}{4}u^2 - v; \end{aligned} \quad (4)$$

We denote the zero temperature values of u and v as u_0 and v_0 , respectively. We take $u_0 = 246$ GeV whereas v_0 is not fixed but variable.

In this model, there are two neutral scalar Higgs bosons. At the tree level, the masses for them are given by

$$\begin{aligned} (m^0)^2; (m_s^0)^2 &= \frac{1}{2} \left[\frac{2}{s} + (3 +)u^2 + (3s +)v^2 - \frac{1}{2} + 2v \right. \\ &\quad \left. - \frac{1}{4} \left[\frac{2}{s} + (3 -)u^2 - (3s -)v^2 - \frac{1}{2} - 2v \right]^2 \right. \\ &\quad \left. + 2v - \frac{1}{2} \right] u^2 \quad \#_{1=2} \quad (5) \end{aligned}$$

We associate the lighter neutral scalar Higgs boson with the real part of the neutral component of the Higgs doublet while the heavier one with the real Higgs singlet S .

At the tree level, the gauge bosons and the top quark masses are $m_W(u_0) = 80.423$ GeV, $m_Z(u_0) = 91.187$ GeV, and $m_t(u_0) = 175$ GeV. They are all defined in terms of u_0 , independently of v_0 .

Now, we consider the one-loop contributions. At the one loop level, the zero temperature effective potential [6] and the finite temperature one [7] are respectively given by

$$V^1(u;v) = \sum_i \frac{n_i}{64} m_i^4(u;v) \log \frac{m_i^2(u;v)}{2} - \frac{3}{2} \sum_i \# \quad (6)$$

$$V^T(u;v) = \sum_i \frac{n_i T^4}{2} \int_0^1 dx x^2 \log [1 - \exp(-x^2 + m_i^2(u;v)/T^2)] \quad (7)$$

where $n_W = 6$, $n_Z = 3$, $n_t = 12$, $n = n_s = 1$ account for the degrees of freedom of each participating particles. In V^1 , we take the renormalization scale as $\mu = 246$ GeV. The negative sign in V^T is for bosons while the positive sign for fermions.

For small $m_i = T$, that is, at high temperature, V^T can be expanded into the well-known form for the temperature induced effective potential. Rather, we perform the integration without using the high temperature approximation in our analysis, in order to consider relatively large scalar Higgs boson mass.

The full effective potential that we consider therefore consists of

$$V(u;v) = V^0(u;v) + V^1(u;v) + V^T(u;v) : \quad (8)$$

Note that the effective Higgs potential possesses a symmetry under interchange $u \leftrightarrow v$. Thus, we may confine ourselves within the region of $u \geq 0$.

In order for the first order electroweak phase transition to take place, we need two separate vacua. The vacua are defined as the points in the (u, v) -plane at which the Higgs potential has local minima. The two extremum conditions for the Higgs potential may be expressed as

$$\frac{\partial V(u;v)}{\partial u} = f_0(u;v) = u f_1(u;v) = 0 ; \quad \frac{\partial V(u;v)}{\partial v} = f_2(u;v) = 0 : \quad (9)$$

where the first equation is decomposed such that it is explicitly satisfied by $u = 0$.

In the above expressions, $f_1(u;v)$ and $f_2(u;v)$ are given as

$$\begin{aligned} f_1(u;v) = & \frac{1}{2} u^2 + \frac{1}{2} v^2 - \frac{m_W^2}{2} + \frac{3m_W^4(u_0)u^2}{8^2 u_0^2} \log \frac{m_W^2(u_0)u^2}{u_0^2} \\ & + \frac{3m_Z^4(u_0)u^2}{16^2 u_0^2} \log \frac{m_Z^2(u_0)u^2}{u_0^2} \\ & + \frac{3m_t^4(u_0)u^2}{4^2 u_0^2} \log \frac{m_t^2(u_0)u^2}{u_0^2} \\ & + \frac{(3 + \frac{1}{2})}{32^2} m_{S_0}^2 \log \frac{m_{S_0}^2}{2} + m_{S_0}^2 \log \frac{m_{S_0}^2}{2} \\ & - \frac{1}{32^2 u_0^2} f(m_{S_0}^2; m_{S_0}^2) - \frac{3T^2 m_W^2(u_0)}{2^2 u_0^2} \int_0^1 dx x^2 d_1(m_W^2) \\ & - \frac{3T^2 m_Z^2(u_0)}{2^2 u_0^2} \int_0^1 dx x^2 d_1(m_Z^2) - \frac{6T^2 m_t^2(u_0)}{2^2 u_0^2} \int_0^1 dx x^2 d_1^+(m_t^2) \\ & - \frac{T^2}{4^2} \int_0^1 dx x^2 d_1(m_{S_0}^2) (3 + \frac{1}{2}) - \frac{1}{(m_{S_0}^2 - m_{S_0}^2)u} \\ & - \frac{T^2}{4^2} \int_0^1 dx x^2 d_1(m_{S_0}^2) (3 + \frac{1}{2}) + \frac{1}{(m_{S_0}^2 - m_{S_0}^2)u} \\ f_2(u;v) = & \frac{1}{2} v + \frac{1}{2} v^3 + \frac{1}{2} v u^2 - \frac{m_W^2}{4} v^2 + \frac{1}{32^2} (3 + \frac{1}{2}) v \\ & - m_{S_0}^2 \log \frac{m_{S_0}^2}{2} + m_{S_0}^2 \log \frac{m_{S_0}^2}{2} - \frac{1}{32^2} f(m_{S_0}^2; m_{S_0}^2) \\ & - \frac{T^2}{4^2} \int_0^1 dx x^2 d_1(m_{S_0}^2) (3 + \frac{1}{2}) v - \frac{1}{(m_{S_0}^2 - m_{S_0}^2)} \\ & - \frac{T^2}{4^2} \int_0^1 dx x^2 d_1(m_{S_0}^2) (3 + \frac{1}{2}) v - \frac{1}{(m_{S_0}^2 - m_{S_0}^2)} ; \quad (10) \end{aligned}$$

with

$$f(a;b) = \frac{1}{(b-a)} \left[a \log \frac{a}{2} - b \log \frac{b}{2} \right] + 1 ; \quad (11)$$

$$f_1 = \frac{1}{2} u^2 + \frac{1}{2} v^2 - \frac{m_W^2}{4v} + v (3 + \frac{1}{2}) u + 2 \frac{1}{2} v - \frac{1}{2} u^2 ;$$

$$d_1(m_i^2) = \frac{2u^2 - 2sv^2 \frac{u^2}{4v} + v \left(3s - \frac{1}{v}\right)v + \frac{1}{4} + 4 - 2v \frac{1}{2} u^2}{\exp \frac{1}{x^2 + m_i^2 = T^2}} : \quad (12)$$

Note that the negative sign in $d_1(m_i^2)$ is for bosons whereas the positive sign is for fermions.

Since the first extremum equation is satisfied by either $u = 0$ or $f_1(u;v) = 0$, one of the two points in the (u, v) -plane which satisfy the two extremum equations is simply $(0, v_1)$ where v_1 is the solution of $f_2(0;v_1) = 0$. This is the vacuum of the unbroken phase state. We solve $f_2(0;v_1) = 0$ to obtain v_1 numerically by the bisection method. Let the other point in the (u, v) -plane which satisfies the two extremum equations be denoted as (u_2, v_2) , where $u_2 \neq 0$. This is the vacuum of the broken phase state. This point is obtained by the Newton's method.

In order to check that the extremum $(u_2;v_2)$ thus obtained is minimum indeed, we need a Jacobian matrix

$$J_{ij}(u;v) = \begin{pmatrix} \frac{\partial f_1(u;v)}{\partial u} & \frac{\partial f_1(u;v)}{\partial v} \\ \frac{\partial f_2(u;v)}{\partial u} & \frac{\partial f_2(u;v)}{\partial v} \end{pmatrix} : \quad (13)$$

This point is a minimum of the Higgs potential if they satisfy $J_{ii} (i=1;2) > 0$ and $\det(J_{ij}) > 0$. The distance between the two minima in the (u, v) -plane is defined as $v_c = \frac{1}{\sqrt{(u_2)^2 + (v_2 - v_1)^2}}$. The nonzero v_c ensures that the electroweak phase transition is discontinuous, that is, first order. The strength of the first order electroweak phase transition is measured by the critical temperature T_c , which is defined as the temperature at which the values of the potential at the two minima are equal: $V(0;v_1) = V(u_2;v_2)$. We determine T_c by varying temperature T until $V(0;v_1) = V(u_2;v_2)$ is met. If the ratio $v_c = T_c$ is larger than 1, the first order electroweak phase transition is defined conventionally as a strong one.

Now, let us evaluate the masses of the two neutral scalar Higgs bosons from the symmetric 2×2 mass matrix at the one-loop level. The masses are evaluated at zero temperature. Thus, V^T does not contribute to the masses at the one-loop level, and we should take $u = u_0$ and $v = v_0$ in the final expressions. The elements of the mass matrix for the neutral scalar Higgs bosons are given by

$$\begin{aligned} M_{11} &= (M_{11}^0 + M_{11}^1) ; \\ M_{22} &= (M_{22}^0 + M_{22}^1) ; \\ M_{12} &= (M_{12}^0 + M_{12}^1) ; \end{aligned} \quad (14)$$

where M_{ij}^0 and M_{ij}^1 are obtained from V^0 and V^1 , respectively. Explicitly, they are obtained as

$$\begin{aligned} M_{11}^0 &= 2u^2 ; \\ M_{22}^0 &= 2sv^2 - v + \frac{u^2}{4v} ; \\ M_{12}^0 &= 2uv - \frac{1}{2}u ; \end{aligned} \quad (15)$$

and

$$M_{11}^1 = \frac{3m_W^4(u)}{4 \cdot 2u^2} \log \frac{m_W^2(u)}{2} + \frac{3m_Z^4(u)}{8 \cdot 2u^2} \log \frac{m_Z^2(u)}{2} + \frac{3m_t^4(u)}{2 \cdot 2u^2} \log \frac{m_t^2(u)}{2}$$

$$\begin{aligned}
& + \frac{1}{32} \frac{g(m_{S_0}^2; m_{S_0}^2)}{(m_{S_0}^2 - m_{S_0}^2)^2} \frac{(3 +)^2 u^2}{16 v^2} f(m_{S_0}^2; m_{S_0}^2) \\
& + \frac{(3 +)^2 u^2}{32} \log \frac{m_{S_0}^2 m_{S_0}^2}{4} + \frac{(3 +) u}{16} \frac{1}{(m_{S_0}^2 - m_{S_0}^2)} ; \\
M_{22}^1 &= \frac{1}{32} \frac{!}{4v} + \frac{1}{v} m_{S_0}^2 \log \frac{m_{S_0}^2}{2} 1 + m_{S_0}^2 \log \frac{m_{S_0}^2}{2} 1 \\
& + \frac{1}{32} \frac{g(m_{S_0}^2; m_{S_0}^2)}{(m_{S_0}^2 - m_{S_0}^2)^2} \frac{3}{32} f(m_{S_0}^2; m_{S_0}^2) \\
& + \frac{1}{32} (3 +) v \frac{!}{4} \log \frac{m_{S_0}^2 m_{S_0}^2}{4} \\
& + \frac{1}{16} (3 +) v \frac{!}{4} \frac{\log(m_{S_0}^2 - m_{S_0}^2)}{(m_{S_0}^2 - m_{S_0}^2)} ; \\
M_{12}^1 &= \frac{1}{32} \frac{g(m_{S_0}^2; m_{S_0}^2)}{(m_{S_0}^2 - m_{S_0}^2)^2} \frac{4}{32} f(m_{S_0}^2; m_{S_0}^2) \\
& + \frac{(3 +) u}{32} (3 +) v \frac{!}{4} \log \frac{m_{S_0}^2 m_{S_0}^2}{4} \\
& + \frac{1}{32} (3 +) v \frac{!}{4} 1 + (3 +) u \frac{1}{2} \frac{\log(m_{S_0}^2 - m_{S_0}^2)}{(m_{S_0}^2 - m_{S_0}^2)} ; \quad (16)
\end{aligned}$$

where

$$g(a; b) = \frac{a + b}{a} \log \frac{b}{a} + 2 ; \quad (17)$$

$$\begin{aligned}
3 &= 2 (3 +) v + \frac{!}{4} + 2 u^2 2 v^2 \frac{! u^2}{4v} + v \frac{!}{4v} \frac{!}{v} \\
&+ 2 \frac{! u^2}{v} ; \\
4 &= 2 (3 +) (3 +) v + \frac{!}{4} u + 8 2 v \frac{!}{2} u : \quad (18)
\end{aligned}$$

In terms of these matrix elements, the neutral scalar Higgs boson masses at the one-loop level are given as

$$m_{S_0}^2; m_S^2 = \frac{1}{2} (M_{11} + M_{22}) \frac{1}{(M_{22} - M_{11})^2 + (M_{12})^2} ; \quad (19)$$

which depend on $\mu, s, v_0, !, \text{ and } v$. Here, it is assumed that $m_{S_0} < m_S$.

For numerical study, we randomly search the parameter space by varying the relevant parameters within the ranges of $0 < \mu; s; 0.7, 0 < v_0 < 300 \text{ GeV}$, and $0 < !; v < 100 \text{ GeV}$. Starting with a set of relevant parameters whose values are chosen randomly within the allowed ranges, we examine if $v_c = T_c > 1$, which is the criterion for the first order electroweak phase transition to be strong. If this criterion is met, we continue to calculate the masses of the neutral scalar Higgs bosons. This sequence of calculations produces a point in the $(\mu, v_c = T_c)$ -plane or in the $(m_S, v_c = T_c)$ -plane. In this way, we perform calculations to obtain 5000 points. Figs. 1a and 1b show the results of our numerical studies on the masses of the neutral

scalar Higgs bosons. In Fig. 1a, the 5000 points thus obtained are plotted in the $(m_s, v_c=T_c)$ -plane, and in Fig. 1b in the $(m_s, v_c=T_c)$ -plane. Notice that the points in the $(m_s, v_c=T_c)$ -plane are scattered slightly toward the right of the plane, as compared to the points scattered in the $(m_s, v_c=T_c)$ -plane, since we assume that $m_s < m_s$. These figures, therefore, indicate that there are sufficiently wide regions in the parameter space where the first order electroweak phase transition is strong as well as the masses of the neutral scalar Higgs bosons are relatively large.

We now examine the possibility of detecting these neutral scalar Higgs bosons in the future linear e^+e^- collider. The three main production processes for the neutral scalar Higgs bosons in e^+e^- collisions are:

$$\begin{aligned} \text{Higgs-strahlung} &: e^+e^- \rightarrow Z \gamma; Z S; \\ \text{W W fusion} &: e^+e^- \rightarrow e^+e^- \gamma; e^+e^- S; \\ \text{Z Z fusion} &: e^+e^- \rightarrow e^+e^- \gamma; e^+e^- S; \end{aligned}$$

where the Higgs-strahlung process is dominant at the center of mass energy corresponding to that of LEP2 whereas W W and Z Z fusion processes are dominant at much higher center of mass energy, such as that of the future linear e^+e^- collider with $\sqrt{s} = 500 \text{ GeV}$.

The cross section for γ or S production via the Higgs-strahlung process is related to the corresponding production cross section of the SM scalar Higgs boson, H , as

$$\begin{aligned} \sigma(Z \gamma) &= \cos^2(\alpha) \sigma_{SM}(ZH \gamma); \\ \sigma(Z S) &= \sin^2(\alpha) \sigma_{SM}(ZH \gamma); \end{aligned} \quad (20)$$

and, similarly, for the W W fusion process, or the Z Z fusion process, one has

$$\begin{aligned} \sigma(VV \gamma) &= \cos^2(\alpha) \sigma_{SM}(VV H \gamma); \\ \sigma(VV S) &= \sin^2(\alpha) \sigma_{SM}(VV H \gamma); \end{aligned} \quad (21)$$

where $VV = W W$ or $Z Z$ and we denote the cross section via the VV fusion process for γ or S production as $\sigma(VV \gamma)$ or $\sigma(VV S)$. Note that the mixing angle α between the two neutral scalar Higgs bosons is introduced above, which is given as

$$\cos(2\alpha) = \frac{M_{11} - M_{22}}{(M_{22} - M_{11})^2 + 4(M_{12})^2} : \quad (22)$$

Since the Higgs-strahlung process is dominant at the center of mass energy of LEP2, we first consider $\sigma(Z \gamma)$ and $\sigma(Z S)$ at $\sqrt{s} = 209 \text{ GeV}$. At this energy, we calculate both $\sigma(Z \gamma)$ and $\sigma(Z S)$ for the same 5000 sets of relevant parameter values which produce the points in Fig. 1a. We take the larger one between $\sigma(Z \gamma)$ and $\sigma(Z S)$ as

$$\sigma_{max}^H = \max[\sigma(Z \gamma); \sigma(Z S)]$$

and plot σ_{max}^H against m_s in Fig. 2. Notice that among the 5000 sets of relevant parameter values, those yielding $m_s > 118 \text{ GeV}$ are excluded kinematically. Thus, there are fewer points in Fig. 2 than in Fig. 1a.

Then, we increase the center of mass energy up to the proposed ILC energy of $\sqrt{s} = 500 \text{ GeV}$. At this energy, the W W and Z Z fusion processes are more dominant than the Higgs-strahlung process for the neutral scalar Higgs productions in e^+e^- collisions. We calculate

$$\begin{aligned} \sigma_{sum}(\gamma) &= \sigma(Z \gamma) + \sigma(W W \gamma) + \sigma(Z Z \gamma); \\ \sigma_{sum}(S) &= \sigma(Z S) + \sigma(W W S) + \sigma(Z Z S); \end{aligned}$$

- [3] A. I. Bochkarev, S. V. Kuzm in, and M. E. Shaposhnikov, *Mod. Phys. Lett. A* 2, 417 (1987); *Phys. Lett. B* 244, 275 (1990); M. Dine, R. G. Leigh, P. Huet, A. Linde, and D. Linde, *Phys. Rev. D* 46, 550 (1992); P. Arnold and O. Espinosa, *Phys. Rev. D* 47, 3546 (1993); Z. Fodor and A. Hebecker, *Nucl. Phys. B* 432, 127 (1994); K. Kajantie, M. Laine, K. Rummukainen, and M. Shaposhnikov, *Phys. Rev. Lett.* 77, 2887 (1996); F. Csikor, Z. Fodor, and J. Heitger, *Phys. Rev. Lett.* 82, 21 (1999).
- [4] A. I. Bochkarev, S. V. Kuzm in and M. E. Shaposhnikov, *Phys. Rev. D* 43, 369 (1991); G. W. Anderson and L. J. Hall, *Phys. Rev. D* 45, 2685 (1992); N. Turok and J. Zadrozny, *Nucl. Phys. B* 369, 729 (1992); G. F. Giudice, *Phys. Rev. D* 45, 3177 (1992); J. R. Espinosa, M. Quiros, and F. Zwimer, *Phys. Lett. B* 307, 106 (1993); K. Enqvist, K. Kainulainen, and I. Vilja, *Nucl. Phys. B* 403, 749 (1993); M. Pietroni, *Nucl. Phys. B* 402, 27 (1993); I. Vilja, *Phys. Lett. B* 324, 197 (1994); A. T. Davies, C. D. Froggatt, G. Jenkins, and R. G. Moorhouse, *Phys. Lett. B* 336, 464 (1994); A. T. Davies, C. D. Froggatt, and R. G. Moorhouse, *Phys. Lett. B* 372, 88 (1996); M. Carena, M. Quiros and C. E. M. Wagner, *Phys. Lett. B* 380, 81 (1996); D. Delepine, J. M. Gerard, R. G. Felipe, and J. Weyers, *Phys. Lett. B* 386, 183 (1996); B. de Carlos and J. R. Espinosa, *Nucl. Phys. B* 503, 24 (1997). J. M. Cline and P. A. Lenioux, *Phys. Rev. D* 55, 3873 (1997); M. Carena, M. Quiros and C. E. M. Wagner, *Nucl. Phys. B* 524, 3 (1998); M. Laine and K. Rummukainen, *Phys. Rev. Lett.* 80, 5259 (1998); *Nucl. Phys. B* 535, 423 (1998); J. M. Cline and G. D. Moore, *Phys. Rev. Lett.* 81, 3315 (1998); K. Funakubo, A. Kakuto, S. Otsuki, and F. Toyoda, *Prog. Theor. Phys.* 99, 1045 (1998); S. J. Huber and M. G. Schmidt, *Eur. Phys. J. C* 10, 473 (1999); K. Funakubo, *Prog. Theor. Phys.* 101, 415 (1999); M. Losada, *Nucl. Phys. B* 537, 3 (1999); M. Bastero-Gil, C. Hugonie, S. F. King, D. P. Roy, and S. Vempati, *Phys. Lett. B* 489, 359 (2000); A. Menon, D. E. Morrissey, and C. E. M. Wagner, *Phys. Rev. D* 70, 035005 (2004); S. W. Ham, S. K. Oh, C. M. Kim, E. J. Yoo, and D. Son, *Phys. Rev. D* 70, 075001 (2004); J. Kang, P. Langacker, T. Li, and T. Liu, [hep-ph/0402086](https://arxiv.org/abs/hep-ph/0402086); M. Carena, A. M. Egevand, M. Quiros, and C. E. M. Wagner, [hep-ph/0410352](https://arxiv.org/abs/hep-ph/0410352).
- [5] J. Choi and R. R. Volkas, *Phys. Lett. B* 317, 385 (1993); J. Choi, *Phys. Lett. B* 345, 253 (1995).
- [6] S. Coleman and E. Weinberg, *Phys. Rev. D* 7, 1888 (1973).
- [7] L. Dolan and R. Jackiw, *Phys. Rev. D* 9, 3320 (1974).

Figure Captions

Fig. 1a : Within the ranges of $0 < \mu_s; \mu_s \leq 0.7$, $0 < v_0 \leq 300$ GeV, and $0 < \lambda; \lambda \leq 100$ GeV, 5000 sets of parameter values are randomly selected which yield $v_c = T_c > 1$, and they are plotted against m_s .

Fig. 1b : For the same 5000 sets of parameter values as in Fig. 1a, $v_c = T_c$ against m_s are plotted.

Fig. 2 : For the same 5000 sets of parameter values as in Fig. 1a, the larger one of the production cross sections, $\sigma_{m_{ax}}^H = \max(\sigma(Z^*); \sigma(Z^*S)g)$, for the neutral scalar Higgs bosons via Higgs-strahlung process in e^+e^- collisions with $\sqrt{s} = 209$ GeV is plotted against m_s . Kinematics for points, that is, those points with $m_s > 118$ GeV are excluded.

Fig. 3a : For the same 5000 sets of parameter values as in Fig. 1a, the production cross section for S via Higgs-strahlung, WW fusion, and ZZ fusion in e^+e^- collisions with $\sqrt{s} = 500$ GeV is plotted against m_s .

Fig. 3b : For the same 5000 sets of parameter values as in Fig. 1a, the production cross section for S via Higgs-strahlung, WW fusion, and ZZ fusion in e^+e^- collisions with $\sqrt{s} = 500$ GeV is plotted against m_s .

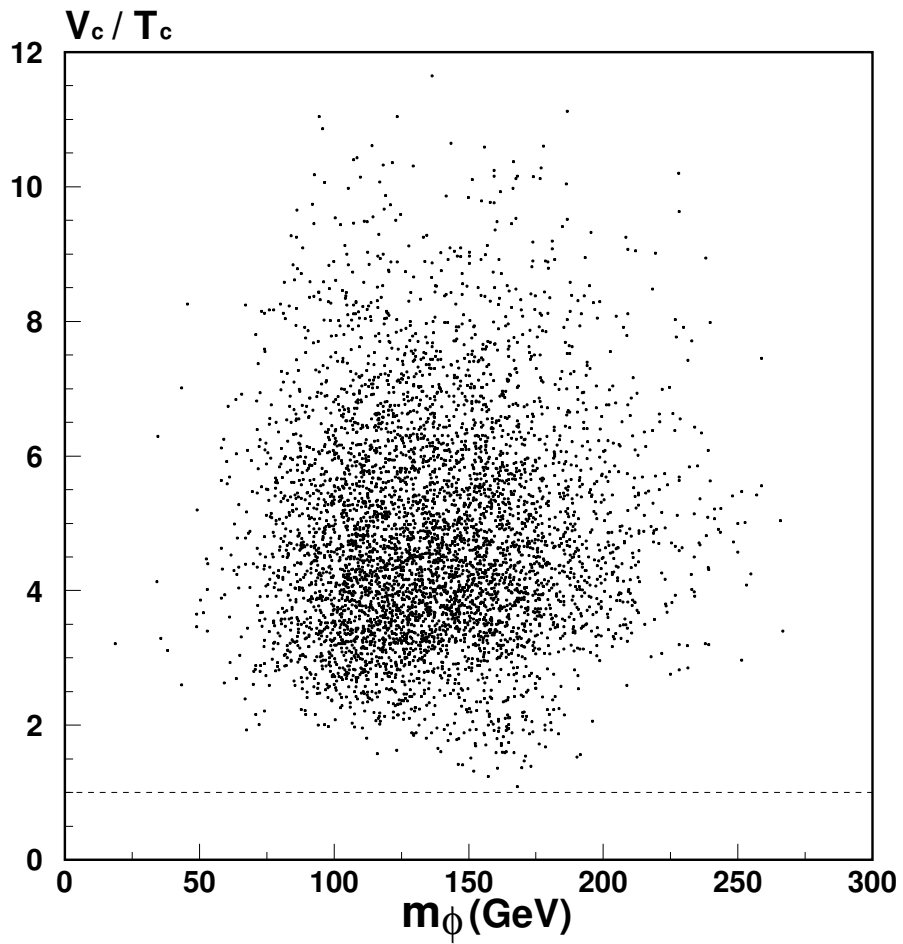


Fig. 1a: Within the ranges of $0 < \dots$; 0.7 , $0 < v_0 \leq 300$ GeV, and $0 < \dots \leq 100$ GeV, 5000 sets of parameter values are randomly selected which yield $v_c/T_c > 1$, and they are plotted against m_ϕ .

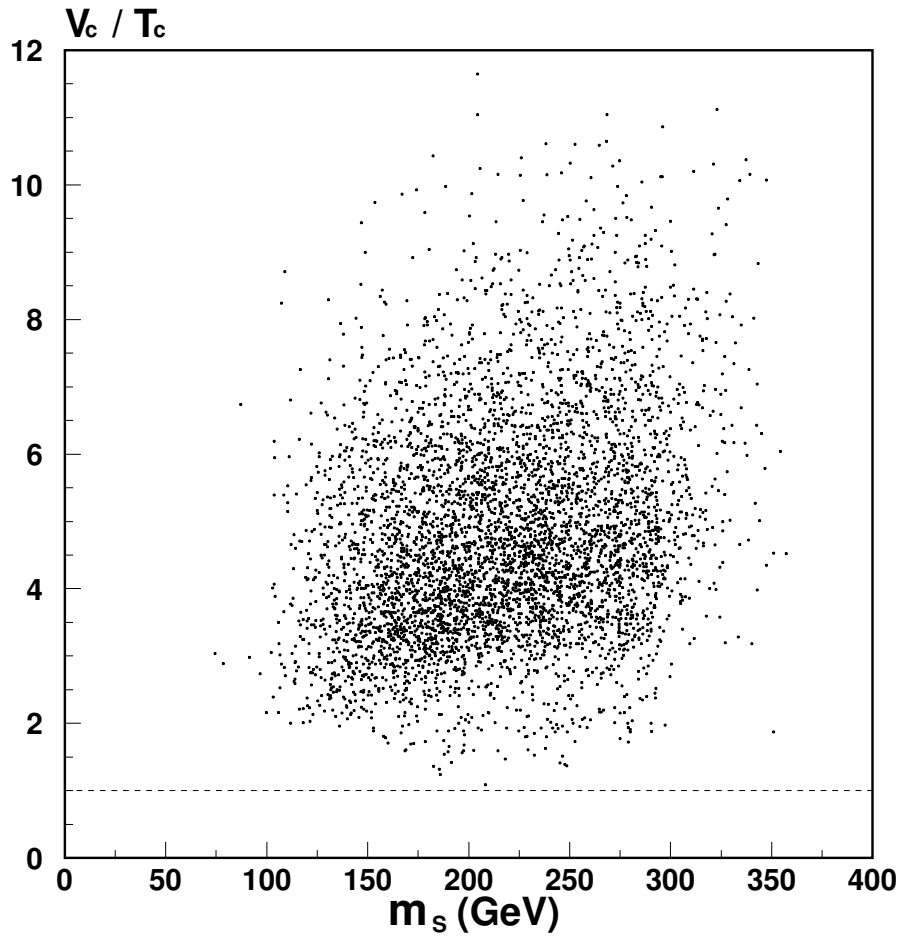


Fig. 1b: For the same 5000 sets of parameter values as in Fig. 1a, $v_c = T_c$ against m_s are plotted.

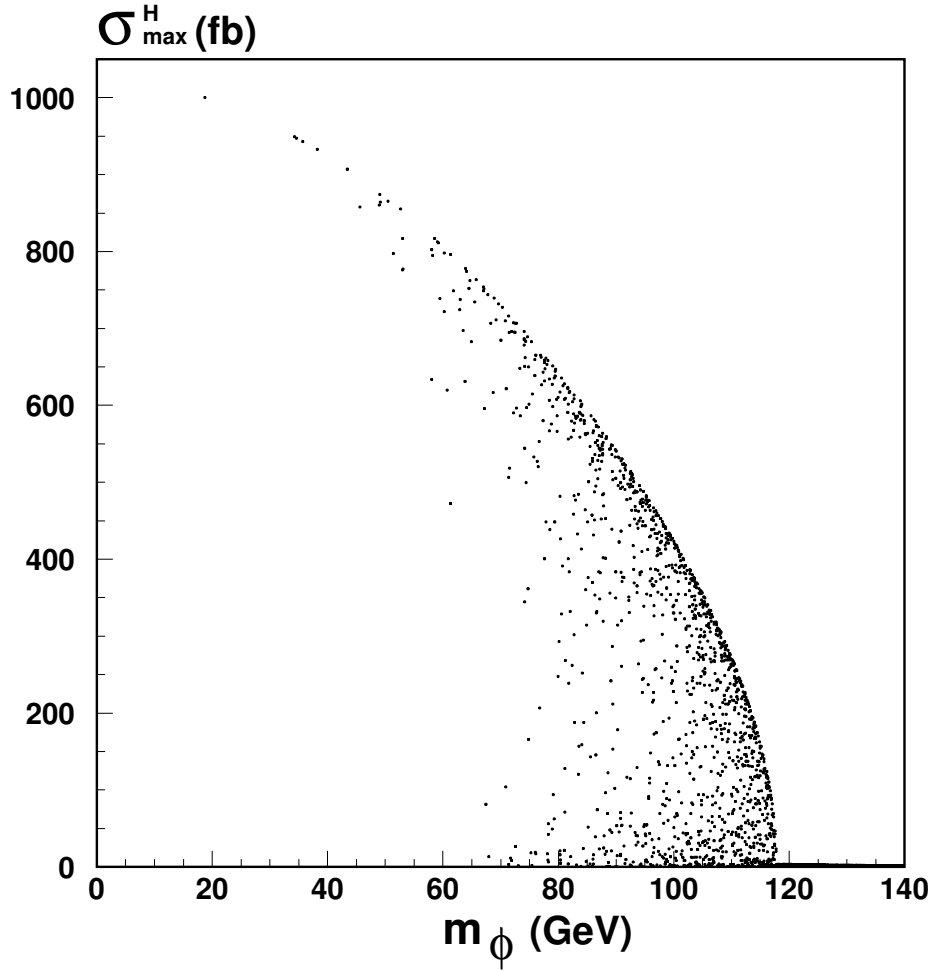


Fig. 2: For the same 5000 sets of parameter values as in Fig. 1a, the larger one of the production cross sections, $\sigma_{\text{max}}^H = \max(\sigma(Z^* \rightarrow Z^* \phi), \sigma(Z^* S)g)$, for the neutral scalar Higgs bosons via Higgs-strahlung process in e^+e^- collisions with $\sqrt{s} = 209$ GeV is plotted against m_ϕ . Kinematics for points, that is, those points with $m_\phi > 118$ GeV are excluded.

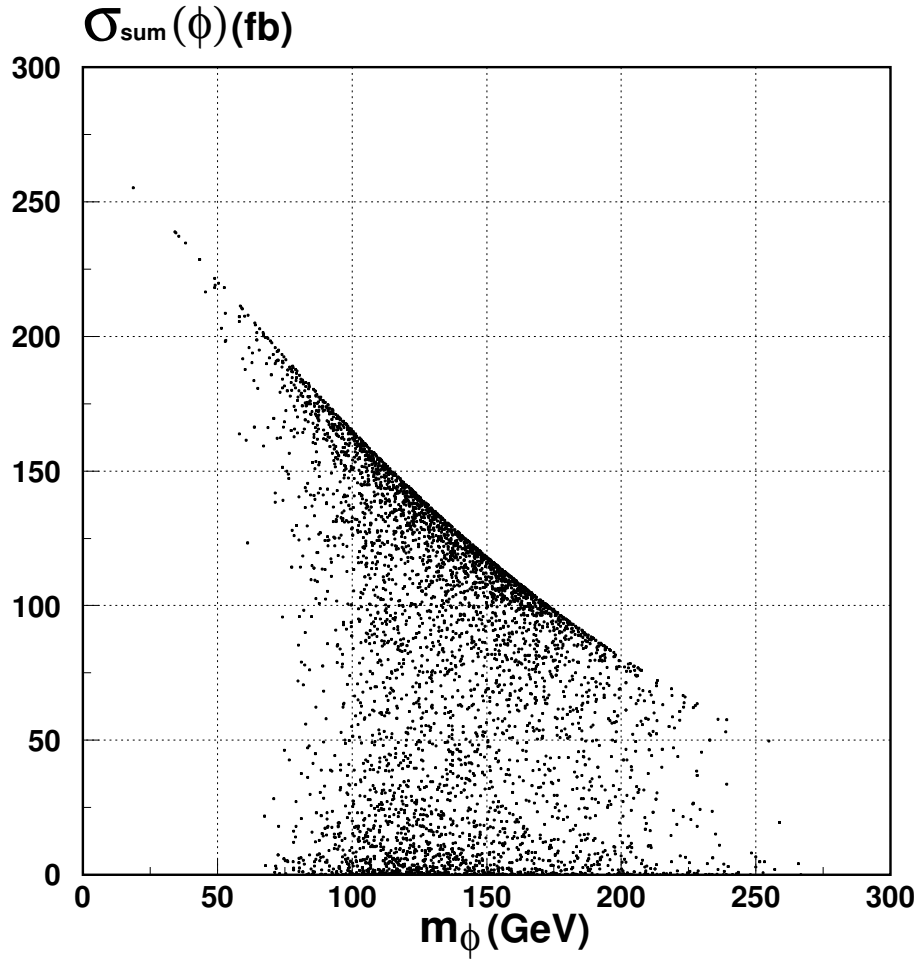


Fig. 3a: For the same 5000 sets of parameter values as in Fig. 1a, the production cross section for ϕ via Higgs-strahlung, $W W$ fusion, and $Z Z$ fusion in $e^+ e^-$ collisions with $\sqrt{s} = 500$ GeV is plotted against m_ϕ .

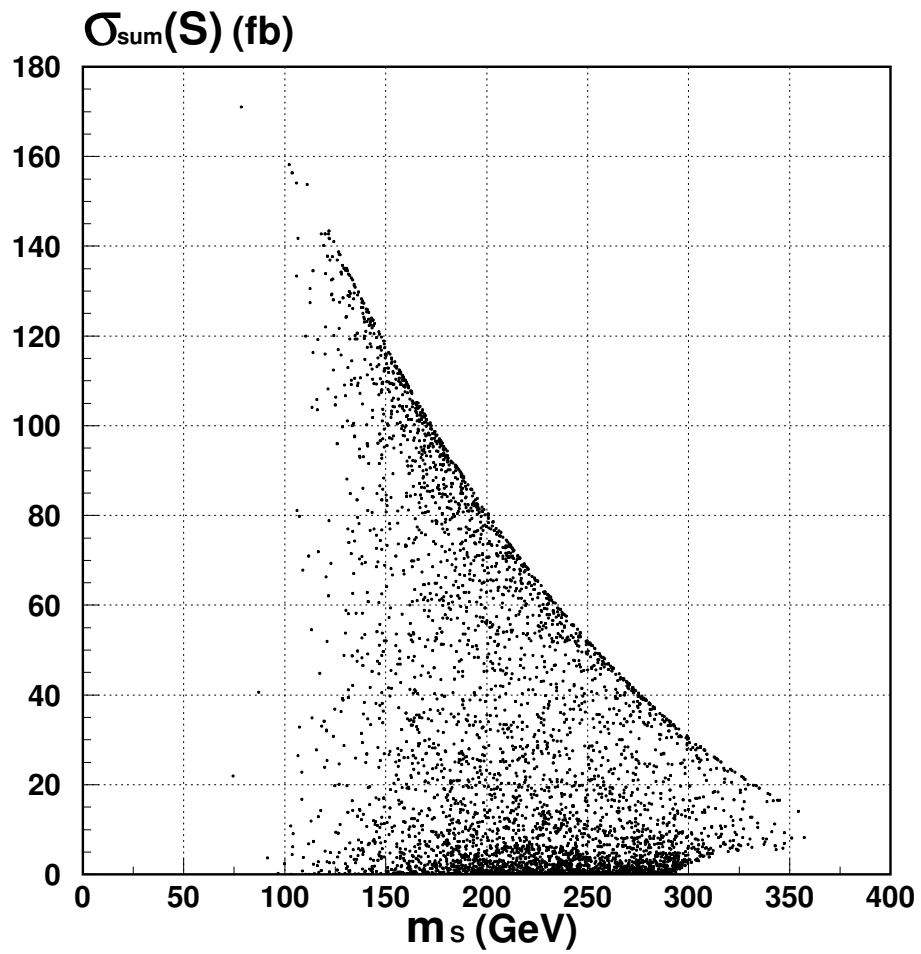


Fig. 3b: For the same 5000 sets of parameter values as in Fig. 1a, the production cross section for S via Higgs-strahlung, WW fusion, and ZZ fusion in e^+e^- collisions with $\sqrt{s} = 500$ GeV is plotted against m_S .